ChemPubSoc Europe
DOI: 10.1002/cctc.201701547
CHEMCATCHEM
Full Papers

VIP *Very Important Paper*

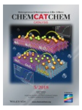

Insight into the Role of Pd State on Pd-Based Catalysts in *o*-Xylene Oxidation at Low Temperature

Yafei Wang,[a, b] Changbin Zhang,*[a, c] and Hong He*[a, c, d]

Pd-based catalysts are long known to be efficient for catalytic oxidation of volatile organic compounds (VOCs), but the effect of the Pd state on the activity remains controversial. In this study, we prepared a series of Pd supported on Co_3O_4, MnO_2, CeO_2, TiO_2, Al_2O_3, SiO_2 catalysts. The as-prepared catalysts were pretreated by $NaBH_4$ and H_2 reduction, respectively, and then tested towards *o*-xylene oxidation. The samples were next characterized to investigate how the Pd state and the support type affect the catalytic activity. The test and characterization results clearly show that the metallic Pd species is much more active than the Pd oxide species for *o*-xylene oxidation at low temperatures, independent of the presence of reducible oxides as supports. Furthermore, $NaBH_4$ pretreatment could avoid undesired support reduction; thus, it is a more appropriate method than H_2 reduction for the preparation of supported metallic noble-metal catalysts.

Introduction

Volatile organic compounds (VOCs) are among the most common air pollutants released by chemical, petrochemical, and related industries. VOCs are the key precursors for the formation of tropospheric ozone and secondary organic aerosols (SOA), leading to serious environmental pollutions.[1] Also, some kinds of VOCs such as benzene derivatives (benzene, toluene, and xylene, BTX) are highly toxic to human health. With the increasingly stringent environmental standards, effective control of VOCs emissions is becoming a very important issue.

Catalytic oxidation is considered to be an effective and environmentally friendly technology for the removal of VOCs owing to its easy application, high efficiency, and no secondary pollution. Noble-metal catalysts are efficient catalysts in the total oxidation of VOCs molecules at low temperatures. Pt, Pd, and a few alloys catalysts are widely investigated for the catalytic oxidation of VOCs.[2] The performance of Pd-based catalysts for VOCs oxidation has been reported to be dependent on many factors,[3] such as Pd loading, Pd particle sizes, Pd state, support type, etc. Although numerous studies have been performed to distinguish the role of each factor, the influencing mechanisms of some factors are still not quite clear. Especially, although the Pd state has been investigated by several researchers, the effect of the Pd state on the catalytic oxidation of VOCs remains controversial. Some authors showed that the metallic species (Pd^0) is more active than the oxide forms (PdO/Pd^{2+}) for catalytic oxidation below 200 °C,[2g, 3d] whereas others affirmed that both species (PdO/Pd^0) are active for oxidation reaction.[2f, 3a, 4] We previously observed that if Pd catalyst was supported on γ-Al_2O_3, the catalytic activity of Pd for *o*-xylene oxidation was considerably dependent on the metallic Pd species below 200 °C.[3c] However, we recently found that the well dispersed PdO species was responsible for the complete catalytic oxidation of *o*-xylene over ordered mesoporous Pd/Co_3O_4 at low temperature (<240 °C),[5] indicating that the influence of the Pd state on activity is also closely related to the support type.

The supports were reported to participate in controlling the Pd amount anchored on the catalyst surface.[6] It has also been found that the supports could be directly involved in the reaction pathway if reducible oxides are employed.[7] In addition, it is shown that both oxidation state and stability of Pd species are closely dependent on the acid–base properties of the supports.[3a] Generally, Pd species loaded on acidic supports are easily oxidized, whereas Pd species supported on basic supports are difficult to oxidize.[3a, f] Therefore, it is necessary to consider employing different supports during preparation, pretreatment, and also oxidation reaction to obtain a better understanding of the effect of the Pd state on the catalytic oxidation of VOCs.

In this study, we prepared Pd supported on a series of oxides such as Al_2O_3, TiO_2, SiO_2, CeO_2, MnO_2, and Co_3O_4. The

---

[a] *Dr. Y. Wang, Prof. C. Zhang, H. He*
Department State Key Joint Laboratory of Environment Simulation and Pollution Control
Research Center for Eco-Environmental Sciences,Chinese Academy of Sciences
Beijing 100085 (China)
E-mail: cbzhang@rcees.ac.cn
honghe@rcees.ac.cn

[b] *Dr. Y. Wang*
Beijing Institute of Petrochemical Technology
Beijing 102617 (China)

[c] *Prof. C. Zhang, H. He*
University of Chinese Academy of Sciences
Beijing 100049 (China)

[d] *H. He*
Center for Excellence in Regional Atmospheric Environment
Institute of Urban Environment,Chinese Academy of Sciences
Xiamen 361021 (China)

The ORCID identification number(s) for the author(s) of this article can be found under:
https://doi.org/10.1002/cctc.201701547.

as-prepared catalysts were pretreated by $NaBH_4$ and H_2 reduction, respectively, and then tested towards the catalytic oxidation of *o*-xylene. The changes of the physicochemical properties of both Pd species and supports were examined by using N_2 physisorption (BET method), powder X-ray diffraction (XRD), and X-ray photoemission spectroscopy (XPS) methods to elucidate how the Pd state and the support affect the catalytic activity. Based on the test and characterization results, we affirm that the metallic Pd species is much more active than the Pd oxide species for *o*-xylene oxidation at low temperatures, independent of the presence of reducible oxides as supports.

Results

Catalytic activity

The PdO/MOx, Pd/MO_x-H_2, and Pd/MO_x-$NaBH_4$ catalysts were tested for the catalytic oxidation of *o*-xylene in the condition of 10% *v*/*v* water vapor, and the results are shown in Figure 1. Without pretreatment, all the PdO/MO_x catalysts exhibited almost no catalytic activities for *o*-xylene oxidation if the reaction temperature was below 190 °C. With increasing temperature, the *o*-xylene conversion was gradually enhanced and reached 100% conversion over PdO/TiO_2, PdO/SiO_2, PdO/CeO_2, and PdO/Al_2O_3 at approximately 250 °C and over PdO/Co_3O_4, and PdO/Mn_2O_3 at approximately 270 °C. After $NaBH_4$ reduction, all the Pd/MO_x-$NaBH_4$ catalysts showed much better activity than the corresponding PdO/MO_x in the temperature range from 110 to 230 °C. Especially, the Pd/MO_x-$NaBH_4$ (Al_2O_3, TiO_2, CeO_2, Mn_2O_3, Co_3O_4) catalysts achieved 100% *o*-xylene conversion at 210 °C. Pd/SiO_2-$NaBH_4$ exhibited 100% conversion of *o*-xylene at 230 °C. In contrast, H_2 reduction exerted a complicated influence on the activity of Pd-based catalysts. The H_2 reduction clearly improved the activities of PdO/MO_x (Al_2O_3, TiO_2, SiO_2, CeO_2) catalysts and shifted the curves of *o*-xylene conversion to lower temperatures, although it showed no promotion on the PdO/Mn_2O_3 catalyst, and Pd/Mn_2O_3-H_2 showed a very similar activity to PdO/Mn_2O_3. Exceptionally, the H_2 reduction dramatically decreased the activity of PdO/Co_3O_4 and shifted the curve of *o*-xylene conversion to higher temperatures. These results suggest that $NaBH_4$ reduction could efficiently improve the catalytic performances of all Pd-based catalysts for *o*-xylene oxidation, whereas the effect of H_2 pretreatment on the Pd-based catalysts was closely dependent on the support type.

XRD and BET analyses

To investigate the reason for the different catalytic behaviors of the reduced catalysts, all samples were characterized by XRD and BET measurements. The XRD patterns of PdO/MO_x, Pd/MO_x-H_2, and Pd/MO_x-$NaBH_4$ catalysts are presented in Figure 2. As shown in Figure 2A, a small PdO peak at $2\theta = 34.3°$ was detected over Al_2O_3 support before the reduction. After H_2 and $NaBH_4$ treatments, the PdO peak disappeared and a small Pd peak at $2\theta = 40.2°$ appeared, indicating that the PdO species were reduced into the metallic Pd species.[8] In contrast, both H_2 and $NaBH_4$ reduction showed no influence on the crystal structure of Al_2O_3 support and all three samples exhibited similar XRD patterns of γ-phase Al_2O_3. As shown in

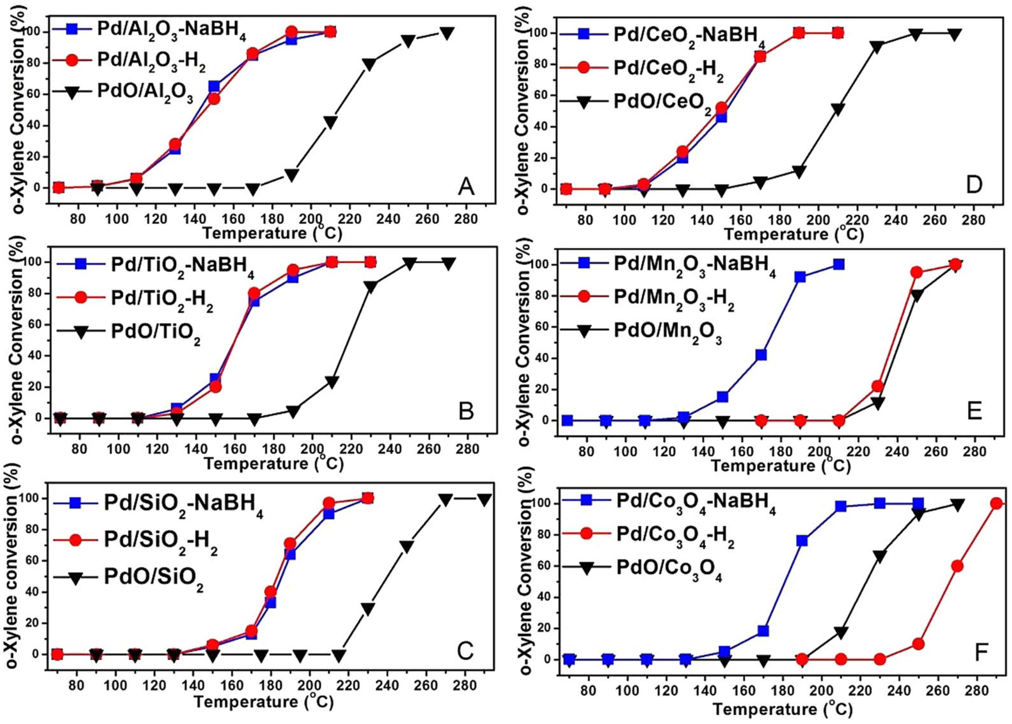

Figure 1. Conversion of *o*-xylene as a function of temperature over PdO/MO_x, Pd/MO_x-H_2, and Pd/MO_x-$NaBH_4$ catalysts in the condition of 10% *v*/*v* water-vapor addition; M = A) Al, B) Ti, C) Si, D) Ce, E) Mn, F) Co.

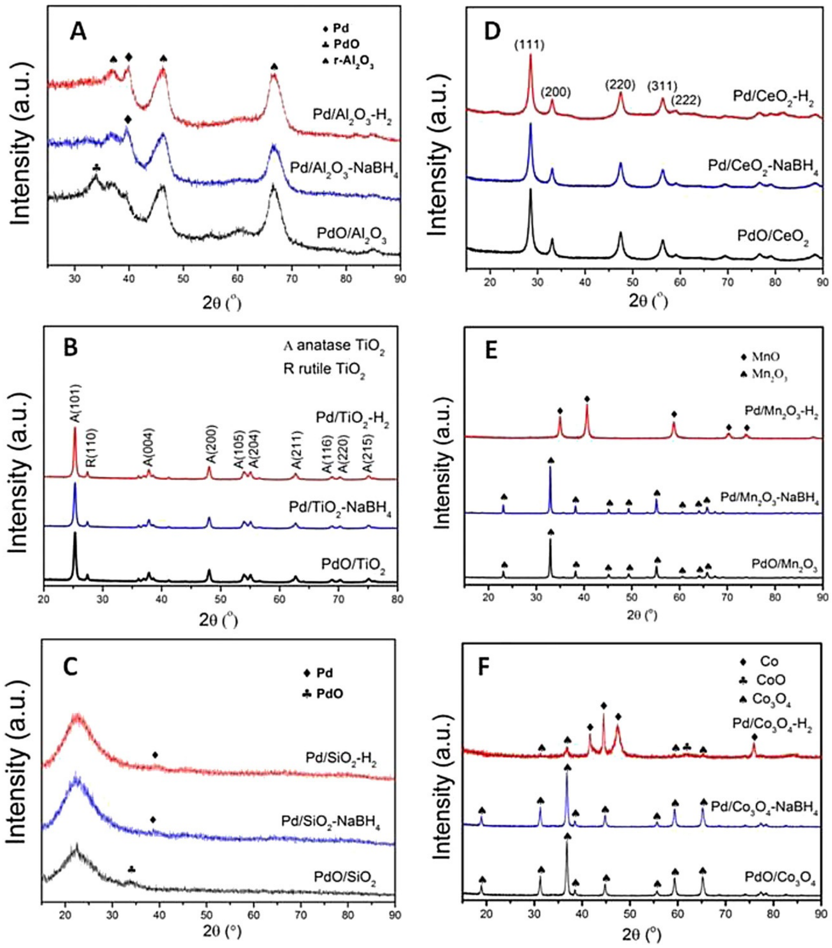

Figure 2. XRD patterns for PdO/MO_x, Pd/MO_x-H_2, and Pd/MO_x-$NaBH_4$ catalysts; M = A) Al, B) Ti, C) Si, D) Ce, E) Mn, F) Co.

Figure 2B,D, the H_2 and $NaBH_4$ treatments showed no influence on the XRD patterns of both TiO_2- and CeO_2-supported catalysts. The samples presented XRD patterns identical to anatase TiO_2 or fluorite-phase CeO_2, respectively. No peaks of PdO or Pd species were observed possibly resulting from their high dispersion on TiO_2 and CeO_2 supports. As for the SiO_2-supported catalysts (Figure 2C), a very samll PdO peak was detected before the two kinds of reduction treatments, which disappeared whereas a weak Pd peak at 40.2° could be observed after H_2 or $NaBH_4$ treatments. Also, both reduction treatments induced no change of the SiO_2 support. As for the Mn_2O_3- and Co_3O_4-supported catalysts (Figure 2E and Figure 2F, respectively), no peaks of PdO and Pd species were observed before and after the reduction treatments. The $NaBH_4$ reduction showed no influence on the XRD patterns of the samples. In contrast, H_2 pretreatment induced dramatic changes of the Mn_2O_3 and Co_3O_4 supports, of which Mn_2O_3 was transformed into MnO, and Co_3O_4 was almost completely reduced into metallic Co.

Based on the XRD patterns, we also calculated the particle sizes of the metallic Pd species over the Pd/Al_2O_3-H_2 and Pd/Al_2O_3-$NaBH_4$ samples according to the peak half-width using the Scherer formula, and the results are given in Table 1. The Pd particle sizes over Pd/Al_2O_3-H_2 and Pd/Al_2O_3-$NaBH_4$ are similar with 7.9 and 7.5 nm, respectively. As the peaks of Pd species over Pd/SiO_2-$NaBH_4$ and Pd/SiO_2-H_2 were very weak, we did not calculate the particle sizes of the Pd species in these two samples.

The specific surface area (S_{BET}), average pore size (d), and total pore volume (V) of all catalysts before and after H_2 and $NaBH_4$ pretreatments were next measured, and the results are also listed in Table 1. The H_2 and $NaBH_4$ pretreatments had little impact on the parameters of Al_2O_3-, TiO_2-, CeO_2-, and SiO_2-supported catalysts, but the H_2 pretreatment sharply decreased the pore sizes and pore volumes of Mn_2O_3 and Co_3O_4 catalysts, which was attributed to the crystal-phase transformation of Mn_2O_3 and Co_3O_4 supports during H_2 reduction.

XPS analysis

The samples were next studied by XPS to obtain the chemical states of the Pd species. The Pd 3d XPS spectra of the Pd-based catalysts are shown in Figure 3. Before reduction, the Pd $3d_{5/2}$ peaks appeared at binding energies ($BE_{Pd\,3d_{5/2}}$) higher than 336.6 eV, indicating that the Pd species mainly existed in the oxidized state[9] over all PdO/MO_x catalysts. After H_2 and $NaBH_4$ pretreatment, the Pd $3d_{5/2}$ peaks shifted to lower BE at

Table 1. Physical properties of the catalysts.

Catalyst	Surface area [$m^2 g^{-1}$]	Average pore size [nm]	Pore volume [$cm^3 g^{-1}$]	Pd particle size [nm]
PdO/Al_2O_3	266	13.7	0.91	–
Pd/Al_2O_3-$NaBH_4$	261	12.7	0.83	7.9
Pd/Al_2O_3-H_2	241	13.9	0.84	7.5
PdO/TiO_2	58	29.3	0.43	–
Pd/TiO_2-$NaBH_4$	58	27.4	0.39	
Pd/TiO_2-H_2	57	28.6	0.42	
PdO/SiO_2	161	3.4	1.38	–
Pd/SiO_2-$NaBH_4$	155	4.0	1.55	–
Pd/SiO_2-H_2	156	3.5	1.37	–
PdO/CeO_2	122	3.6	0.11	
Pd/CeO_2-$NaBH_4$	120	3.6	0.11	
Pd/CeO_2-H_2	121	3.7	0.11	
PdO/Mn_2O_3	17	29.6	0.13	
Pd/Mn_2O_3-$NaBH_4$	22	29.7	0.16	
Pd/Mn_2O_3-H_2	16	11.7	0.05	
PdO/Co_3O_4	29	17.4	0.20	
Pd/Co_3O_4-$NaBH_4$	39	17.3	0.31	
Pd/Co_3O_4-H_2	22	3.3	0.17	

approximately 335.0 eV, which is attributed to the metallic Pd species,[10] demonstrating that both H_2 and $NaBH_4$ treatment could effectively reduce the Pd oxides into metallic Pd species over these catalysts.

The chemical states of the oxide supports are presented in Figure 4, and the calculated elemental components are summarized in Table 2. Clearly, TiO_2, Al_2O_3, SiO_2, and CeO_2 (Figure 4A–D) showed the almost identical XPS spectra before and after the two reductions, confirming that the H_2 and $NaBH_4$ pretreatments have no much influence on their chemical states. In contrast, as shown in Figure 4E,F, the $NaBH_4$ pretreatment caused only little change of the Mn 2p and Co 2p XPS spectra, whereas the H_2 pretreatment shifted the peaks of Mn 2p and Co 2p XPS to lower binding energies. The Mn 2p XPS peaks in PdO/Mn_2O_3 and Pd/Mn_2O_3-$NaBH_4$ were located at approximately 641.7 eV, which belongs to Mn_2O_3.[11] After H_2 reduction, the Mn 2p peak appeared at 641.2 eV, which is ascribed to Mn^{2+}, showing that the Mn_2O_3 was reduced into MnO.[12] The XPS spectra of Co were curve-fitted, and the results are shown in Figure 4F and summarized in Table 2. The Co^{3+} (779.6 eV) and Co^{2+} (781.1 eV) species coexisted on the PdO/Co_3O_4 catalyst,[13] and their percentages were 67 % and 33 %, respectively. The $NaBH_4$ pretreatment showed no clear effect on the chemical state of Co species and only caused a slight change of the Co^{3+} and Co^{2+} percentage (63 % Co^{3+} and 37 % Co^{2+}). The H_2 pretreatment induced a dramatic change of the Co_3O_4 chemical state, and the Co^{3+} was completely reduced to Co^{2+} or Co^0. The percentages of Co^{2+} and Co^0 were 29 % and 71 %, respectively.

Discussion

Based on the XRD and XPS results, it was shown that H_2 and $NaBH_4$ pretreatments both could reduce PdO into metallic Pd species on all tested supports (Al_2O_3, TiO_2, SiO_2, CeO_2, Mn_2O_3, and Co_3O_4). $NaBH_4$ pretreatment exhibited no influence on crystal structures and chemical states of the supports even though CeO_2, Mn_2O_3, and Co_3O_4 are reducible. The test results

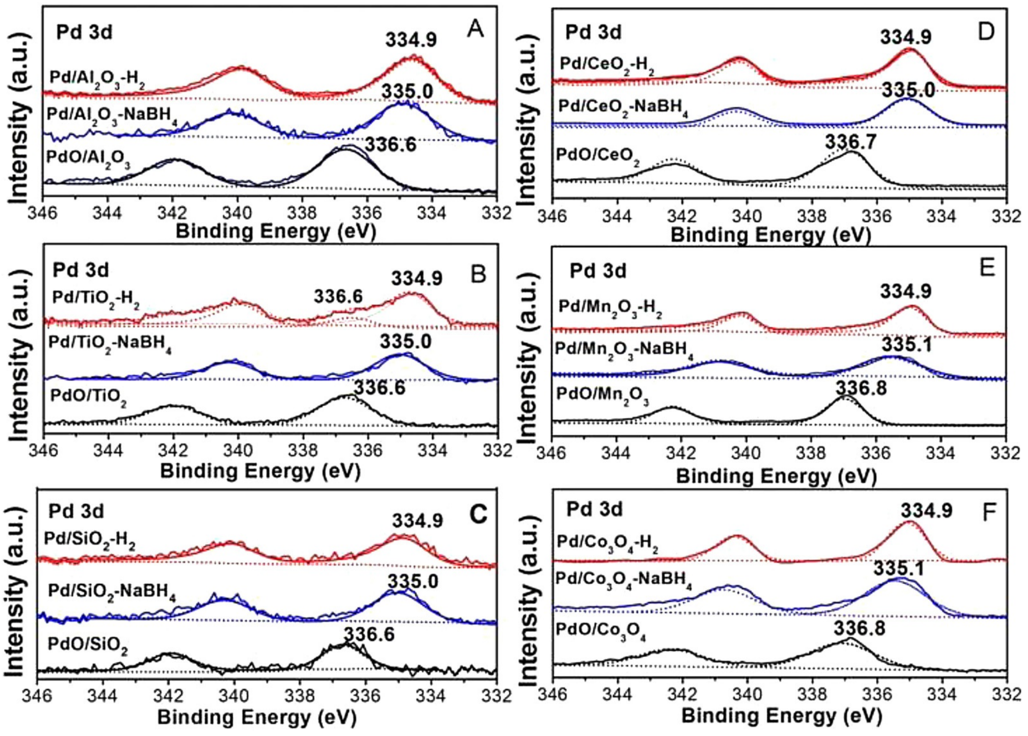

Figure 3. Pd 3d XPS spectra of PdO/MO_x, Pd/MO_x-H_2, and Pd/MO_x-$NaBH_4$ catalysts; A) Al, B) Ti, C) Si, D) Ce, E) Mn, F) Co.

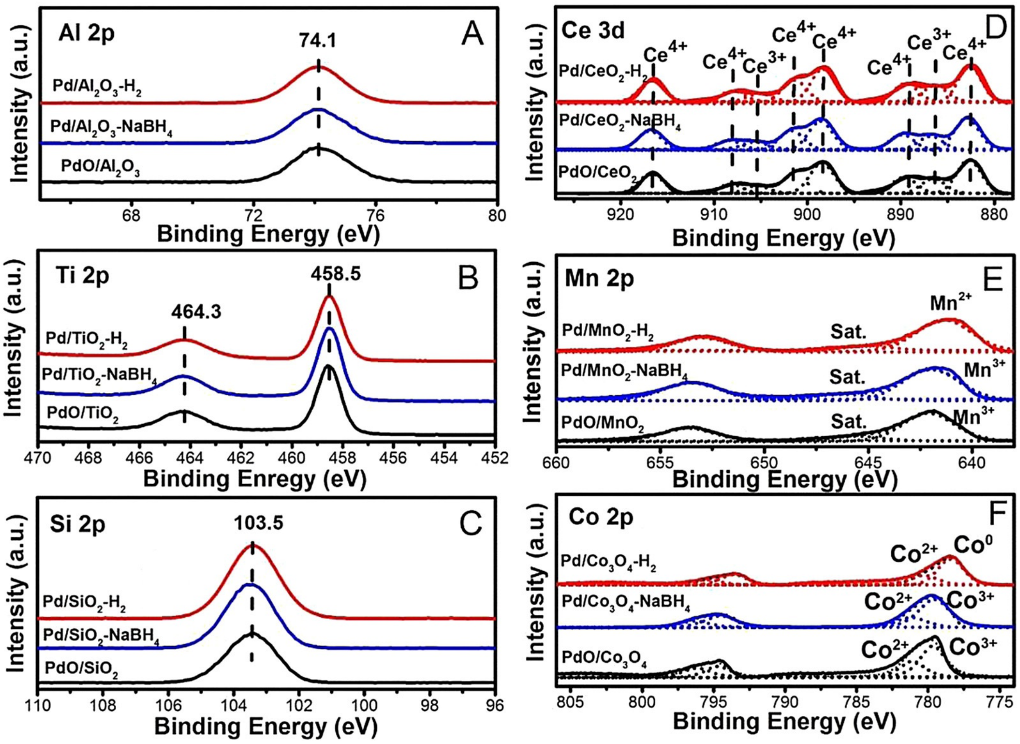

Figure 4. XPS spectra of the supports with different pretreatments; A) Al 2p, B) Ti 2p, C) Si 2p, D) Ce 3d, E) Mn 2p, F) Co 2p.

Table 2. Element components on catalyst surfaces calculated based on XPS spectra.

Catalyst	Element	Peak [eV]	FWHM	Component [%]
PdO/Al_2O_3	Al	74.1($2p_{3/2}$)	2.03	Al_2O_3(100)
Pd/Al_2O_3-$NaBH_4$		74.1($2p_{3/2}$)	2.06	Al_2O_3(100)
Pd/Al_2O_3-H_2		74.1($2p_{3/2}$)	1.99	Al_2O_3(100)
PdO/TiO_2	Ti	458.5($2p_{3/2}$)	1.11	TiO_2(100)
Pd/TiO_2-$NaBH_4$		458.5($2p_{3/2}$)	1.11	TiO_2(100)
Pd/TiO_2-H_2		458.5($2p_{3/2}$)	1.12	TiO_2(100)
PdO/SiO_2	Si	103.5($2p_{3/2}$)	1.78	SiO_2(100)
Pd/SiO_2-$NaBH_4$		103.5($2p_{3/2}$)	1.76	SiO_2(100)
Pd/SiO_2-H_2		103.5($2p_{3/2}$)	1.80	SiO_2(100)
PdO/CeO_2	Ce[a]	886.4($3d_{5/2}$)	2.91	Ce^{3+}(14.4)
		882.5($3d_{5/2}$)	2.16	Ce^{4+}(85.6)
Pd/CeO_2-$NaBH_4$		886.4($3d_{5/2}$)	2.87	Ce^{3+}(14.6)
		882.5($3d_{5/2}$)	2.13	Ce^{4+}(85.4)
Pd/CeO_2-H_2		886.4($3d_{5/2}$)	2.90	Ce^{3+}(14.3)
		882.5($3d_{5/2}$)	2.14	Ce^{4+}(85.7)
PdO/Mn_2O_3	Mn	641.7($2p_{3/2}$)	2.57	Mn_2O_3(100)
		646.2($2p_{3/2}$)	2.96	Sat.
Pd/Mn_2O_3-$NaBH_4$		641.7($2p_{3/2}$)	2.54	Mn_2O_3(100)
		646.2($2p_{3/2}$)	2.98	sat.
Pd/Mn_2O_3-H_2		641.2($2p_{3/2}$)	2.27	MnO(100)
		645.3($2p_{3/2}$)	2.91	sat.
PdO/Co_3O_4	Co	779.6($2p_{3/2}$)	2.21	Co_2O_3(67)
		781.2($2p_{3/2}$)	2.12	CoO(33)
Pd/Co_3O_4-$NaBH_4$		779.6($2p_{3/2}$)	2.16	Co_2O_3(63)
		781.1($2p_{3/2}$)	2.65	CoO(37)
Pd/Co_3O_4-H_2		780.3($2p_{3/2}$)	2.25	CoO(29)
		778.4($2p_{3/2}$)	2.14	Co(71)

[a] The surface atomic concentration of Ce^{3+} and Ce^{4+} were calculated by the curve-fitted Ce 3d XPS spectra.

(Figure 1) showed that each of the Pd/MO_x samples reduced by $NaBH_4$ treatment is much more active than the unreduced sample, indicating that the metallic Pd species is the active site for the catalytic oxidation of *o*-xylene at low temperature range. The H_2 pretreatment showed no influence on the crystal structures of Al_2O_3, TiO_2, CeO_2, and SiO_2 supports; therefore, the Pd/Al_2O_3-H_2, Pd/TiO_2-H_2, Pd/ CeO_2-H_2, and Pd/SiO_2-H_2 samples exhibited the much higher activities than the unreduced ones, further confirming that the metallic Pd species is the active center. In contrast, H_2 treatment induced a dramatic change of crystal structures and chemical states of the Mn_2O_3 and Co_3O_4 supports. Therefore, even though H_2 reduction effectively reduced PdO into metallic Pd on Mn_2O_3 and Co_3O_4 supports, the activities of Pd/Mn_2O_3-H_2 and Pd/Co_3O_4-H_2 samples were not enhanced; on the contrary, the H_2 reduction sharply dropped the activity of Pd/Co_3O_4-H_2 catalyst, indicating that the support was also involved in the catalytic oxidation reaction over Pd-based catalysts.

If the Pd species are in the metallic state and the supports keep their physicochemical properties, the Pd particle size will be a key factor affecting the catalytic activity.[14] As shown in Table 1, the Pd particle sizes over Pd/Al_2O_3-H_2 are similar to those over Pd/Al_2O_3-$NaBH_4$; therefore, these two catalysts showed similar activities.

H_2 treatment is the most commonly used method to reduce a metal oxide into its metallic state, especially for the preparation of supported noble-metal catalysts. The above results show that H_2 treatment could induce changes in the crystal structures and chemical states of some reducible metal oxides that were employed as supports. As both Pd species and support have a great influence on the catalyst activity, the changes in the support properties introduced by the reduction step make it more difficult to estimate the role of the Pd state in catalysis. This is one of the reasons for the long-time controversy about the effect of Pd state on activity. In contrast, $NaBH_4$ treatment, which is performed at room temperature, could only reduce the PdO_x into the metallic Pd species, but showed no capacity to reduce the support oxides. Therefore, the $NaBH_4$ reduction should be a better way for the preparation of supported metallic noble-metal catalysts.

Conclusions

We have found that reduced Pd species on metal-oxide (Al_2O_3, TiO_2, SiO_2, CeO_2, MnO_2, Co_3O_4) supported Pd catalysts are much more active for the complete oxidation of *o*-xylene in the temperature range 90–230 °C than PdO_x. To the best of our knowledge, it is thus confirmed for the first time that the metallic Pd species are the active sites for the oxidation of volatile organic compounds at low temperatures. The previous confusion about the effect of Pd valence states on the activity therefore mainly resulted from the reduction-induced changes of the valence state or crystal structure of the support. In addition, we found that $NaBH_4$ pretreatment avoids undesired support reduction; therefore, it is a more appropriate method than H_2 reduction for the preparation of metallic noble-metal supported-catalysts.

Experimental Section

Catalyst preparation

TiO_2 was commercially available Degussa P25 and SiO_2 was purchased from Aldrich (99.9% purity). And γ-Al_2O_3 was prepared from boehmite (AlOOH, Shandong Aluminum Corporation) by calcining at 600 °C for 3 h. Co_3O_4, MnO_2, and CeO_2 were synthesized by homogeneous precipitation method with urea as the precipitator. Typically, the aqueous solutions of the precursors and excessive urea aqueous solution were mixed. The mixed solution was then heated to 90 °C and held there for 12 h with vigorous stirring. After filtration and washing with deionized water, the resulting precipitates were dried at 100 °C overnight and subsequently calcined at 400 °C for 6 h in air conditions.

The 1 wt.% Pd-supported catalysts were then prepared by impregnation of the supports with aqueous $Pd(NO_3)_2$ (Aldrich) for 1 h. After impregnation, the excess water was removed in a rotary evaporator at 60 °C. The samples were dried at 110 °C for 12 h and then calcined at 400 °C for 6 h. The as-prepared samples were denoted PdO/MO_x. The PdO/MO_x catalysts were further pretreated by H_2 reduction to obtain the reduced samples (denoted Pd/MO_x-H_2). For the H_2 reduction process, the PdO/MO_x catalysts were treated in a flow of H_2 at 50 $mL\,min^{-1}$ for 60 min at 300 °C for PdO/MO_x (Al_2O_3, TiO_2, SiO_2, and CeO_2) catalysts and at 200 °C for PdO/MnO_2 and PdO/Co_3O_4 catalysts. In addition, the reduced catalysts were also prepared by $NaBH_4$ reduction process. The oxide powders were dispersed in deionized water and then a certain amount of aqueous $Pd(NO_3)_2$ was added into the suspension. Next, a $NaBH_4$ aqueous solution as reducing agent was added into the mixture of $Pd(NO_3)_2$ and MO_x ($NaBH_4/Pd = 10$, molar ratio) at room temperature under stirring for 1 h. After filtration and washing with deionized water, the samples were dried at 60 °C overnight without further calcination. The obtained samples were denoted as Pd/MO_x-$NaBH_4$.

Catalyst characterization

Power XRD analysis was used to identify the crystalline phases present in the catalysts. A Bruker D8 Advance diffractometer with monochromatic $Cu_{K\alpha}$ source operated at 40 kV and 40 mA was used. The specific surface areas, pore sizes, and volumes of the catalysts were measured at −196 °C using a Quantachrome Quadrasorb SI-MP analyzer. Prior to the N_2 physisorption, the catalysts were degassed at 300 °C for 5 h. Specific surface areas were calculated from the isotherms by applying the BET equation in the 0.05–0.30 partial pressure range. XPS measurements were recorded on a Scanning X-ray Microprobe (AXIS Ultra, Kratos Analytical, Inc.). The binding energy was calibrated with C 1s = 284.8 eV.

Catalytic activity tests

The catalytic activities of the catalysts were evaluated in a continuous-flow fixed-bed quartz microreactor between 70 and 300 °C with 100 mg of the catalyst. The reactant feed (flow rate = 100 $mL\,min^{-1}$) was composed of 150 ppm *o*-xylene, 10% H_2O and air, with the weight hour space velocity (WHSV) of 60 000 $mL\,g^{-1}\,h^{-1}$. The outlet gas was analyzed online by a GC–MS (Agilent 6890-5973 N, HP-5MS) and a GC (Shangfen GC-112A, TDX-01 column).

Acknowledgements

This work was financially supported by the National Key R&D Program of China (2017YFC0211802, 2016YFC0207104), the National Natural Science Foundation of China (21422706, 21577159) and the Youth Innovation Promotion Association, CAS (2017064).

Conflict of interest

The authors declare no conflict of interest.

Keywords: oxidation · heterogeneous catalysis · palladium · reduction · supported catalysts

[1] a) C. Huang, H. L. Wang, L. Li, Q. Wang, Q. Lu, J. A. de Gouw, M. Zhou, S. A. Jing, J. Lu, C. H. Chen, *Atmos. Chem. Phys.* **2015**, *15*, 11081 – 11096; b) H. M. Parikh, A. G. Carlton, Y. Zhou, H. Zhang, R. M. Kamens, W. Vizuete, *Atmos. Environ.* **2012**, *56*, 250 – 260.

[2] a) G. Avgouropoulos, E. Oikonomopoulos, D. Kanistras, T. Ioannides, *Appl. Catal. B* **2006**, *65*, 62 – 69; b) F. J. Maldonado-Hódar, C. Moreno-Castilla, A. F. Pérez-Cadenas, *Appl. Catal. B* **2004**, *54*, 217 – 224; c) M. N. Padilla-Serrano, F. Maldonado-Hodar, C. Moreno-Castilla, *Appl. Catal. B* **2005**, *61*, 253 – 258; d) J. Requies, M. C. Alvarez-Galvan, V. L. Barrio, P. L. Arias, J. F. Cambra, M. B. Guemez, A. M. Carrera, V. A. D. la Peha O'Shea, J. L. G. Fierro, *Appl. Catal. B* **2008**, *79*, 122 – 131; e) L. F. Wang, T. P. Tran, D. V. Vo, M. Sakurai, H. Kameyama, *Appl. Catal. A* **2008**, *350*, 150 – 156; f) H. Tan, J. Wang, S. Yu, K. Zhou, *Environ. Sci. Technol.* **2015**, *49*, 8675 – 8682; g) C. Zhang, Y. Li, Y. Wang, H. He, *Environ. Sci. Technol.* **2014**, *48*, 5816 – 5822.

[3] a) K. Okumura, T. Kobayashi, H. Tanaka, M. Niwa, *Appl. Catal. B* **2003**, *44*, 325–331; b) P. G. Tsyrul'nikov, T. N. Afonasenko, S. V. Koshcheev, A. I. Boronin, *Kinet. Catal.* **2007**, *48*, 728–734; c) S. Huang, C. Zhang, H. He, *Catal. Today* **2008**, *139*, 15–23; d) S. Huang, C. Zhang, H. He, *J. Environ. Sci.* **2013**, *25*, 1206–1212; e) S. C. Kim, W. G. Shim, *Appl. Catal. B* **2009**, *92*, 429–436; f) K. Okumura, M. Niwa, *Catal. Surv. Jpn.* **2002**, *5*, 121–126.

[4] a) J. M. Padilla, G. Del Angel, J. Navarrete, *Catal. Today* **2008**, *133*, 541–547; b) T. Zheng, J. He, W. Xia, H. Hochstadt, J. Yang, Y. Zhao, *Catal. Commun.* **2015**, *71*, 51–55; c) K. Okumura, S. Matsumoto, N. Nishiaki, M. Niwa, *Appl. Catal. B* **2003**, *40*, 151–159.

[5] Y. Wang, C. Zhang, F. Liu, H. He, *Appl. Catal. B* **2013**, *142*, 72–79.

[6] a) S. Colussi, A. Gayen, M. F. Camellone, M. Boaro, J. Llorca, S. Fabris, A. Trovarelli, *Angew. Chem. Int. Ed.* **2009**, *48*, 8481–8484; *Angew. Chem.* **2009**, *121*, 8633–8636; b) K. Zhou, Y. Li, *Angew. Chem. Int. Ed.* **2012**, *51*, 602–613; *Angew. Chem.* **2012**, *124*, 622–635; c) J. A. Farmer, C. T. Campbell, *Science* **2010**, *329*, 933–936.

[7] a) V. M. Belousov, M. A. Vasylyev, L. V. Lyashenko, N. Y. Vilkova, B. E. Nieuwenhuys, *Chem. Eng. J.* **2003**, *91*, 143–150; b) N. Acerbi, S. Golunski, S. C. Tsang, H. Daly, C. Hardacre, R. Smith, P. Collier, *J. Phys. Chem. C* **2012**, *116*, 13569–13583.

[8] Y. Kang, X. Ye, C. B. Murray, *Angew. Chem. Int. Ed.* **2010**, *49*, 6156–6159; *Angew. Chem.* **2010**, *122*, 6292–6295.

[9] a) M. Shen, G. Wei, H. Yang, J. Wang, X. Wang, *Fuel* **2013**, *103*, 869–875; b) Y. Lu, Y. Jiang, X. Gao, X. Wang, W. Chen, *J. Am. Chem. Soc.* **2014**, *136*, 11687–11697.

[10] J. He, I. Ichinose, T. Kunitake, A. Nakao, Y. Shiraishi, N. Toshima, *J. Am. Chem. Soc.* **2003**, *125*, 11034–11040.

[11] R. K. Kunkalekar, A. V. Salker, *React. Kinet. Mech. Catal.* **2012**, *106*, 395–405.

[12] *Handbook of X-Ray Photoelectron Spectroscopy* (Eds.: C. D. Wagner, W. M. Riggs, G. E. Muilenberg), Perkin-Elmer Corp., Physical Electronics Division, Eden Prairie, Minnesota, USA, **1979**.

[13] L. F. Liotta, G. Di Carlo, A. Longo, G. Pantaleo, A. M. Venezia, *Catal. Today* **2008**, *139*, 174–179.

[14] D. Gao, H. Zhou, J. Wang, S. Miao, F. Yang, G. Wang, J. Wang, X. Bao, *J. Am. Chem. Soc.* **2015**, *137*, 4288–4291.

Manuscript received: September 25, 2017
Revised manuscript received: October 19, 2017
Accepted manuscript online: October 19, 2017
Version of record online: January 17, 2018